NASA Technical Paper 1735

Experimental Study of Cluster Formation in Binary Mixture of H_2O and H_2SO_4 Vapors in the Presence of an Ionizing Radiation Source

Jag J. Singh and Alphonso C. Smith
Langley Research Center
Hampton, Virginia

Glenn K. Yue
Institute for Atmospheric Optics and Remote Sensing
Hampton, Virginia

National Aeronautics
and Space Administration

**Scientific and Technical
Information Branch**

1980

A

SUMMARY

The molecular clusters formed in laboratory-grade pure nitrogen containing H_2O and H_2SO_4 vapors and exposed to a 3-mCi Ni^{63} beta source have been studied in the mass range 50 to 780 amu using a quadrupole mass spectrometer. Measurements were made under several combinations of relative humidity (R.H.) and relative acidity (R.A.) in the ranges 0.7 to 7.5 percent (R.H.) and 0.00047 to 0.06333 percent (R.A.). Several H_2O and H_2SO_4 molecular clusters of the form $(H_2SO_4)_{N_A} \cdot (H_2O)_{N_B} \cdot H^+$ were detected for each R.H./R.A. combination. The relative intensities of the molecular clusters detected for a certain R.H./R.A. combination changed as R.A. and/or R.H. were changed. The number of H_2SO_4 molecules in the clusters ranged from 1 to 7, whereas the number of H_2O molecules ranged from 1 to 16. Classical binary nucleation theory calculations, including the effects of ions present in the reaction chamber, indicate that stable and transient clusters of the type detected would be formed under the experimental conditions used in this study. However, the predicted cluster mass spectrum does not agree with the experimentally observed spectra for any of the R.H./R.A. combinations. The experimental clusters are much larger than the calculated cluster sizes. This discrepancy may be the result of inaccuracies in the values of the surface tension and the effective charge of the clusters used in the calculations. The first factor arises from the fact that a macroscopic value of the surface tension appropriate for a liquid phase (H_2SO_4 + H_2O) has been used in the calculations instead of a value more appropriate for small molecular clusters. The second effect arises by virtue of the fact that the H_2O molecule has a permanent dipole moment and the H_2SO_4 molecule has a significant electrical polarizability. First-order calculations using modified surface tension values and including the effects of multipole moments of the nucleating molecules indicate that these effects may be enough to explain the disagreement between the calculated and the measured cluster spectra.

INTRODUCTION

Several recent studies have shown that the surfaces of environmental aerosols are enriched in a number of trace elements, some of which are known to be toxic. Jolly and coworkers (ref. 1) studied size-differentiated aerosols and found that S, Ca, Fe, Zn, Sn, and Pb are concentrated preferentially in the surfaces of the aircraft exhaust aerosols. Singh and coworkers (ref. 2) studied size-dependent composition of aerosols emitted from oil-fired heating plants and noted that Zn, Mo, Ag, and Pb have a tendency to concentrate preferentially in the smaller aerosols (i.e., exhibit preference for surface residence). Aerosols from municipal incinerators have been shown (ref. 3) to have an excess of K, S, Mn, and Ni in the aerosol surfaces. Aerosols emitted from coal-fired plants have been reported (ref. 4) to have surface enrichment in Cr, K, Mn, Na, Pb, S, Tl, V, and Zn, but not in Al, Ca, Fe, Mg, Si, and Ti. More recent studies by Singh and Khandelwal (ref. 5) have shown that fly ash derived from combustion of eastern coal in a conventional power plant has a multimodal size distribution

with different modes having different elemental compositions. These findings suggest that different types of aerosols present in power plant emission are formed by quite different processes. The excess of Fe, K, Ca, and Ti in the 4.0-μm size group is attributable to deposition of volatile compounds of these elements onto the surfaces of combustion aerosols as the temperature decreases up the exhaust stack. The excess of sulphur in submicrometer aerosols was explained by heteromolecular nucleation such as $2\ NH_3 + H_2SO_4 \rightarrow (NH_4)_2SO_4$ and $n(H_2O) + m(H_2SO_4) \rightarrow H_2SO_4$ (dilute) at the stack top. Keyser and coworkers (ref. 4) studied auto exhaust aerosols and found two distinct morphological forms. The first, involving larger particles, exhibited an excess of Pb, Br, Cl, and S at the particle surfaces whereas the second form involved submicrometer spherical particles composed exclusively of Pb, Br, and Cl. The homogeneous nature of smaller spherical particles suggests that their formation occurs by a nucleation process in which PbBrCl condenses to form quite pure molten droplets when the temperature outside the exhaust system falls below the saturation point.

It thus appears that gas-to-particle phase conversion may play an important role in the formation of submicrometer aerosols in high-temperature combustion sources - such as coal-fired power plants and auto engine exhausts. Abrupt changes in the temperature, pressure, and relative humidity encountered outside the combustion zone may facilitate homogeneous heteromolecular nucleation process, even though the condensation of volatile vapors on the existing aerosol surfaces is known to be a strong competitor. However, large numbers of charged species present[1] in the combustion exhaust may provide centers of attraction to form aerosols through ion-induced heteromolecular nucleation process.

Theoretical considerations (refs. 6 to 9) and limited experimental results (refs. 10, 11, and 12) available demonstrate that ultrafine aerosols can be formed by heteromolecular nucleation under suitable environmental conditions. However, the structure of these aerosols, whose size at the nucleation time is only of the order of a few angstroms, has not been studied well experimentally. It is believed that the molecular structure of these ultrafine aerosols is a critical test of the classical liquid drop theory of nucleation process discussed in the section "Theoretical Background."

If was therefore decided to simulate, in a reaction chamber, the relevant environmental conditions encountered in a combustion exhaust and to study the formation of ultrafine aerosols, using a quadrupole mass spectrometer. The first set of experiments involved gaseous H_2O and H_2SO_4 mixtures and an ionizing radiation source. The values of relative humidity and relative acidity[2] in the reaction chamber were controlled so as to provide, for the most part, a stable region for the cluster formation. The results of these initial experiments are discussed in this paper.

---

[1]It is possible that Coulomb forces may play an important role, due to the polar nature of the molecular species involved in many of the high-temperature combustion reactions, even in the absence of ionic reactants.

[2]Relative acidity is defined as the ratio of the ambient vapor pressure to the saturation vapor pressure of H_2SO_4, with the latter values at various temperatures having been taken from references 13 and 14.

SYMBOLS

e	elementary charge
ΔG	Gibbs free energy
k	Boltzmann constant
M_A, M_B	molecular weight of component A or B
N_A, N_B	number of molecules of species A or B
n_A, n_B	number of moles of component A or B in embryo
P_A, P_B	environmental vapor pressure of component A or B
P_A^{sol}, P_B^{sol}	equilibrium partial vapor pressure of A or B over flat surface of solution
P_{N_A, N_B}	probability of ion clusters containing N_A molecules of A and N_B molecules of B
Q	charge of cluster
R	universal gas constant
R.A.	relative acidity
R.H.	relative humidity
r	radius of embryo
r_o	radius of ion core
T	temperature of reaction chamber, absolute units
ϵ	dielectric constant of cluster
ρ	density of mixture
σ	surface tension of mixture in embryo
σ_{mac}	macroscopic surface tension

THEORETICAL BACKGROUND

The molecular interaction and subsequent aerosol formation in the reaction chamber can be described as follows:

The Gibbs free energy ΔG of formation of liquid embryos in a binary gas mixture in the absence of any ionization source is given by the following equation (ref. 15):

$$\Delta G = -n_A RT \ln \frac{P_A}{p_A^{sol}} - n_B RT \ln \frac{P_B}{p_B^{sol}} + 4\pi r^2 \sigma \tag{1}$$

where

$n_{A,B}$	number of moles of component A or B in embryo
R	universal gas constant
T	temperature of reaction chamber, absolute units
$P_{A,B}$	environmental vapor pressure of component A or B
$p_{A,B}^{sol}$	equilibrium partial vapor pressure of A or B over flat surface of solution
r	radius of embryo
σ	surface tension of mixture in embryo

As shown by Heist and Reiss (ref. 15), a plot of ΔG as a function of n_A and n_B in three-dimensional space exhibits a saddle point which corresponds to the minimum height of the free energy barrier. Once a cluster reaches the radius corresponding to the saddle point, it is nucleated and can grow to a larger droplet. The radius and the composition of the cluster at this point are called critical values. These values can be obtained as follows. At the saddle point,

$$\left.\begin{aligned} \left[\frac{\partial \Delta G}{\partial n_A}\right]_{n_B} &= 0 \\ \left[\frac{\partial \Delta G}{\partial n_B}\right]_{n_A} &= 0 \end{aligned}\right\} \tag{2}$$

Applying this criterion to equation (1), one obtains the following equations (ref. 16):

$$\ln \frac{P_A}{p_A^{sol}} = \frac{2}{RT} \frac{M_A}{\rho} \frac{\sigma}{r} \left(1 + \frac{x}{\rho} \frac{d\rho}{dx} - \frac{3}{2} \frac{x}{\sigma} \frac{d\sigma}{dx}\right) \tag{3}$$

$$\ln \frac{P_B}{P_B^{sol}} = \frac{2}{RT} \frac{M_B}{\rho} \frac{\sigma}{r} \left(1 - \frac{100 - x}{\rho} \frac{d\rho}{dx} + \frac{3}{2} \frac{100 - x}{\sigma} \frac{d\sigma}{dx} \right) \tag{4}$$

where

ρ density of mixture

$M_{A,B}$ molecular weight of component A or B

Equations (3) and (4) are called generalized Kelvin equations. Whenever numerical values of n_A and n_B are known, the size and composition of the embryo can be obtained by simply solving equations (3) and (4). Numerical values of P_A^{sol}, P_B^{sol}, σ, and ρ at various temperatures are available for certain compositions in standard references (refs. 13, 17, and 18). Their values for any other composition can be easily calculated by interpolation. The values of P_A and P_B in the reaction chamber can be controlled such that the mass number of the embryo is within the range of the mass spectrometer ($\gtrsim$780 amu, in the present instance).

In the case of ionized interacting species, as is expected to be the case in high-temperature combustion exhausts, equation (1) should be modified to include an extra term due to electrostatic effects, as follows:

$$\Delta G = -n_A RT \ln \frac{P_A}{P_A^{sol}} - n_B RT \ln \frac{P_B}{P_B^{sol}} + 4\pi r^2 \sigma + \frac{Q^2}{2} \left(1 - \frac{1}{\epsilon} \right) \left(\frac{1}{r} - \frac{1}{r_o} \right) \tag{5}$$

where

Q charge on cluster

ϵ dielectric constant of cluster

r_o radius of ion core

If it is assumed that $\epsilon \gg 1$ and $r^3 \gg r_o^3$, substitution of equation (5) in equation (2) yields the following equations (ref. 8):

$$\ln \frac{P_A}{P_A^{sol}} = \frac{2}{RT} \frac{M_A}{\rho} \frac{\sigma}{r} \left[\left(1 - \frac{Q^2}{16\pi\sigma r^3} \right) \left(1 + \frac{x}{\rho} \frac{d\rho}{dx} \right) - \frac{3}{2} \frac{x}{\sigma} \frac{d\sigma}{dx} \right] \tag{6}$$

$$\ln \frac{P_B}{P_B^{sol}} = \frac{2}{RT} \frac{M_B}{\rho} \frac{\sigma}{r} \left[\left(1 - \frac{Q^2}{16\pi\sigma r^3} \right) \left(1 - \frac{100 - x}{\rho} \frac{d\rho}{dx} \right) + \frac{3}{2} \frac{100 - x}{\sigma} \frac{d\sigma}{dx} \right] \tag{7}$$

It has been demonstrated in reference 9 that the sulphate aerosols formed through the ion-induced nucleation process can be classified as stable, transitory, or unstable depending on the values of P_A and P_B in the reaction chamber. Since the stable aerosols are of the order of a few angstroms, they can be detected with a mass spectrometer with a high degree of accuracy and constitute a critical test of the liquid drop model of nucleation. Very little experimental work has been reported about the size and composition of these stable ultrafine aerosol clusters. Most of the reported studies (refs. 10, 11, and 12) deal with the measurement of aerosol nucleation rate (i.e., the number of aerosols formed per unit volume per unit time). Some reported studies have inferred the cluster sizes from the measured values of their mobility and do not attempt to provide information about the composition of the clusters (ref. 10). A mass spectrometric measurement, on the other hand, should provide information about the mass and composition of the clusters formed in ion-molecule and molecule-molecule collisions.

In practice, even in the stable region, more than one type of clusters will be observed. However, the most probable type will be the one for which the free energy is a minimum. The probability p of existence of ion clusters containing N_A molecules of the species A and N_B molecules of species B is given by the following expression:

$$P_{N_A,N_B} = \frac{\exp\left(- \frac{\Delta G(N_A,N_B)}{kT} \right)}{\sum_{i,j} \exp\left(- \frac{\Delta G(i,j)}{kT} \right)} \tag{8}$$

This expression has been used to calculate relative probabilities for various compositions of the $(H_2SO_4)_{N_A} \cdot (H_2O)_{N_B} \cdot H^+$ microclusters.

EXPERIMENTAL PROCEDURE AND RESULTS

Figure 1 shows a schematic diagram of the experimental system used in the present study. Laboratory-grade pure nitrogen (99.998 percent) was used as the carrier gas to introduce predetermined ratios of H_2SO_4 and H_2O vapors into the reaction chamber. The reaction chamber is made up of two cylindrical sections of pyrex glass and a flexible (bellowed) metal section. The larger pyrex section has a diameter of 15.24 cm (6.0 in.) and length of 19.05 cm (7.5 in.)

whereas the smaller section has a diameter of 3.81 cm (1.5 in.) and length of 10.16 cm (4.0 in.). The flexible metal section has a diameter of 3.81 cm (1.5 in.) and length of 10.16 cm (4.0 in.). The free end of the metal section is connected to the mass spectrometer by a 25-μm-diameter collimator. The source region is located at the end of the flexible metal section nearest to the collimator separating the reaction chamber from the mass spectrometer. With this experimental arrangement, the pressure in the mass spectrometer was $\sim 10^{-5}$ torr (a rather high value for the mass spectrometer). (1 torr = 1.3×10^2 Pa.) However, it was necessary to use a pressure ≥ 50 torr in the reaction chamber to produce a sufficient number of positive ions for initiating nucleation. A 3-mCi Ni^{63} beta source was used to produce positive ions in front of the collimator.[3] (1 Ci = 3.7×10^{10} Bq.) The primary ionization products in the source region would be N_2^+ and the ions of the trace components (H_2O and H_2SO_4). However, given sufficient time to react, the terminal positive ions would almost entirely be of the form $H^+ \cdot (H_2O)_N$ where N can vary from zero to a larger number, although some $(N_2)_N$ and $H^+ \cdot (H_2O) \cdot (N_2)_N$ may also be observed (refs. 19, 20, and 21). It is the dominant $H^+ \cdot (H_2O)_N$ ions that are believed to nucleate almost all of the $(H_2SO_4)_{N_A} \cdot (H_2O)_{N_B} \cdot H^+$ microclusters in the source region. The microclusters formed have to travel a distance of approximately 2 mm outside the source region before entering the mass spectrometer region. The mean free path for N_2 molecules in the reaction chamber at a pressure of 1/3 atm (1 atm = 1.013×10^5 Pa) is of the order of 10^{-4} mm, resulting in a large number of collisions between N_2 molecules and the microclusters outside the source region, before they leave the reaction chamber. There may be additional collisions as the carrier gas and the microclusters expand into the mass spectrometer vacuum. Some of these collisions may lead to a modification of the primary clusters, i.e., some clusters may increase or decrease in mass depending on the nature of the colliding partners. However, collisions between primary microclusters are less likely than collisions between the carrier gas molecules and the primary microclusters. The latter collisions can only cause fractionation of the primary clusters. Thus, the experimentally observed cluster spectrum may contain a larger number of smaller clusters than the primary cluster spectrum produced in the source region. The microclusters were detected using a Cu-Be electron multiplier and a picoammeter. Because of the presence of H_2SO_4 in the nucleation clusters, the electron multiplier had to be replaced frequently - usually after a continuous use for a period of approximately 1 month. The spectrometer was calibrated using SF_6 and perfluorotributylamine test gases.

The room temperature and the temperature, pressure, and relative humidity in the reaction chamber were monitored continuously during the measurements. A conventional dewpoint hygrometer was used to measure the moisture content in

---

[3]The choice of the Ni^{63} source was dictated by its low beta end-point energy and its ability to withstand the high temperature needed to bake out the reaction chamber.

the reaction chamber. There have been some reports (ref. 22 and refs. cited therein) indicating that the performance of a dewpoint hygrometer is a function of the H_2SO_4 vapor content of the environment. No definitive evidence of water dewpoint dependence on the rather low H_2SO_4 content of the gas mixture in the reaction chamber was found in the present study. The calculated values of R.H. in the reaction chamber were always higher than the measured values. This was interpreted to imply that the carrier gas bubbling through H_2O did not become saturated at the flow rate used in this study. It was therefore decided to use the measured value of the moisture content, rather than the calculated values which are based on the assumption that the carrier gas after bubbling through a water column would be saturated with moisture. On the other hand, the calculated values of H_2SO_4 concentration were found to be in reasonable agreement with the measured values based on a $BaCl_2 + H_2SO_4 \rightarrow BaSO_4 + 2\ HCl$ pH test. Hence, it was decided to use the calculated values of H_2SO_4 vapor concentration, particularly since there is no quick and simple way of measuring H_2SO_4 concentration in the reaction chamber.[4]

The nucleation spectra were measured for several combinations of R.A. and R.H., summarized in table I. Most of the R.A./R.H. combinations studied provided a stable region for cluster formation in the reaction chamber (ref. 9). Figure 2 shows a typical cluster mass spectrum. The values of R.A. and R.H. in the reaction chamber were 0.0018 percent and 1.6 percent, respectively. Several clusters of the type $(H_2SO_4)_{N_A} \cdot (H_2O)_{N_B} \cdot H^+$ with $N_A = 1$ to 6 and $N_B = 1$ to 15 are present in the spectrum. No cluster spectrum was observed when the Ni^{63} radiation source was shielded from the reaction chamber. This result clearly shows that the nucleation rate is strongly influenced by the ions produced by the radioactive beta source.

An examination of table I shows that the R.A./R.H. combinations studied fall in two broad groups: group I, where R.H. is held constant and R.A. is allowed to change, and group II, where R.A. is held constant and R.H. is allowed to change.

Figures 3 to 5 illustrate the cluster spectra observed under several combinations of R.A. and R.H. values. In general, the increasing acidity of the reaction chamber gas mixture tends to increase the intensity of the clusters with a larger number of H_2SO_4 molecules in them, whereas the increasing humidity tends to increase the H_2O content of the molecular clusters.

COMPARISON WITH THEORY

Typical comparison between the theory and the experiment is exemplified by a discussion of the results shown in figure 2. The clusters observed in

---

[4]It should perhaps be noted that the carrier gas bubbling rate through H_2SO_4 was very low ($\lesssim$ ml/min), thus providing ample time for saturation. On the other hand, the carrier gas bubbling rate through the water column was higher ($\gtrsim$100 ml/min), thereby allowing insufficient time for saturation.

this figure fall in the following broad groups in descending order of intensity (the first number within the brackets represents the number of H_2SO_4 molecules, the second number represents the number of H_2O molecules, and the third number represents the H^+ ion in the cluster):

Group 1	(5,x,1)	Group 4	(4,x,1)
Group 2	(1,x,1)	Group 5	(3,x,1)
Group 3	(2,x,1)	Group 6	(6,x,1)

The experimental cluster size spectrum is summarized in table II(a).

The calculated cluster groups under the same environmental conditions, in descending order of intensity, are as follows:

Group 1	(1,x,1)
Group 2	(2,x,1)

The calculated cluster size spectrum is summarized in table II(b).

It is clear from tables II(a) and II(b) that the observed cluster sizes are considerably larger than the predicted sizes for the selected R.A. and R.H. combination. This discrepancy could result from the following factors:

(a) The numerical values of the surface tension for the cluster, used in calculating stable cluster size, may be inappropriate. The surface tension values used in calculating the results summarized in table II(b) are the macroscopic values for the liquid phase corresponding to the particular cluster compositions. It is not obvious a priori whether the macroscopic liquid phase value of the surface tension is appropriate for a cluster containing only 20 or less molecules.

(b) The electrostatic term for the distributed charges in the cluster may be inadequate. Calculations assume the cluster to be a spherical drop with a unit charge. However, the cluster, most likely, is not spherical and the electrostatic term in the expression for Gibbs free energy does not take account of the fact that the H_2O molecule has a permanent dipole moment and the H_2SO_4 molecule has a high value of electrical polarizability. The calculations thus underestimate the electrostatic effects and hence the cluster size.

(c) Because of rather high pressure in the reaction chamber, multiple collisions involving primary clusters after leaving the source region may lead to larger secondary clusters. However, as has been discussed earlier, collisions between primary clusters are less likely than collisions between the carrier gas (N_2) molecules and the primary clusters. The latter collisions can only cause fractionation of primary clusters yielding yet smaller sizes. It would thus appear that the causes of discrepancy between the theory and the experiment lie in factors (a) and (b). It should, of course, be pointed out that neither coalesence nor fractionation effects have been included in the theoretical calculations.

In order to estimate the possible importance of the above-stated factors, calculations of cluster spectra were made, for the same R.A./R.H. combinations as in figure 2, for the following special cases:

I(a) $Q = 1e$ (where e is the elementary charge)

(b) $Q = 2e$

The value of surface tension used in these calculations was $\sigma = \sigma_{mac}$ (where σ_{mac} is the macroscopic surface tension).

II(a) $\sigma = 1/2\ \sigma_{mac}$

(b) $\sigma = (2\sigma_{mac})^{\dagger}$

The value of the electrostatic charge in the cluster was taken to be $Q = 1e$ in these calculations.

III(a) $Q = 2e$

(b) $\sigma = 1/2\ \sigma_{mac}$

This combination of values of Q and σ was selected since it appeared to predict the cluster mass spectrum closest to the observed data.

The results of these calculations are summarized in tables III to VII. Table III clearly shows that increasing the effective charge in the clusters increases the cluster size, i.e., the number of H_2SO_4 and H_2O molecules in the cluster goes up with the increasing cluster charge. Similarly, the decreasing value of the surface tension leads to an increasing cluster size, whereas an increase in the surface tension value reduces the cluster size (table IV). As seen from tables V to VII, combining the higher value of the effective charge with the lower value of the surface tension predicts large clusters of the types (5,x,1), (6,x,1), (7,x,1), and (8,x,1). Except for certain smaller members of (5,x,1) and (6,x,1) groups, most of these clusters fall outside the mass range of the detection system used. However, secondaries produced by the fractionation of all the clusters predicted would be detected if their mass falls in the experimentally detectable range. Thus, it is quite possible that the experimentally observed cluster spectrum summarized in table II(a) is not inconsistent with the prediction of the modifed classical nucleation theory ($\sigma = 1/2\ \sigma_{mac}$; $Q = 2e$).

---

†Ordinarily, one would expect (refs. 23, 24, and 25) the microscopic surface tension value to be less than the bulk values. However, a value of $\sigma = 2\sigma_{mac}$ has been included in the calculations for emphasizing the effects of changing surface tension on the microcluster spectrum.

From these comparisons, it can be concluded that more appropriate values of σ and Q in equation (5) may lead to much larger nucleation clusters, in agreement with those observed experimentally. It should, of course, be remembered that the experimental cluster spectrum is complicated by the fact that the collision between the primary clusters and the carrier gas molecules may result in the breakup of some of the clusters providing smaller secondary clusters. Thus it would be necessary to incorporate these collision-induced fractionation effects in the calculated spectra before a direct comparison with the experiment can be made.

CONCLUDING REMARKS

A detailed study of ion-induced nucleation in binary mixtures of H_2O and H_2SO_4 gases has been conducted. There is strong experimental evidence that the presence of positive ions in the mixture accelerates the nucleation process greatly. The presence of clusters formed by $H^+(H_2O)$ ion attaching itself to H_2SO_4 and H_2O molecules was first detected by Bricard and coworkers with mobility measurement technique. The present study is probably the first direct detection of $(H_2SO_4)_{N_A} \cdot (H_2O)_{N_B} \cdot H^+$ ions with a mass spectrometer. A determination of the cluster mass provides direct information about its composition, which is believed to be a critical test of the liquid drop model of nucleation. On the basis of the experimental results discussed in this paper, the following broad conclusions can be drawn about the classical theory of ion-induced nucleation in H_2O and H_2SO_4 binary mixtures:

(1) The macroscopic surface tension value for the $(H_2SO_4 + H_2O)$ liquid is not appropriate for the $(H_2SO_4)_{N_A} \cdot (H_2O)_{N_B} \cdot H^+$ nucleation clusters. This, of course, is not surprising in view of the very small size of the nucleation clusters.

(2) The effective charge on the $(H_2SO_4)_{N_A} \cdot (H_2O)_{N_B} \cdot H^+$ clusters is not the unit positive charge carried by the H^+ or $(H_3O)^+$ ion. Experimental data indicate a value closer to two units of charge, suggesting the importance of dipole moments of H_2O and H_2SO_4 (induced) molecules. Perhaps a more accurate treatment of electrostatic potential would include the effects of distributed charges in the cluster. Calculations based on modified values of surface tension and the cluster charge do indicate the importance of these factors in determining the nucleation cluster spectrum.

(3) The necessity of maintaining high pressure ($\bar{>}$50 torr) in the reaction chamber introduces complications caused by multiple collisions involving the clusters and the carrier gas molecules. These complications include fractionation as well as coalescence of the primary clusters, leading to secondary clusters of quite different sizes. The calculated cluster spectra must there-

fore include the fractionation/coalescence effects before they can be compared with the experimental cluster spectra.

Langley Research Center
National Aeronautics and Space Administration
Hampton, VA 23665
September 8, 1980

REFERENCES

1. Jolly, R. K.; Gupta, S. K.; Randers-Pehrson, G.; Buckle, D. C.; Thornton, W. B.; Aceto, H., Jr.; Singh, Jag J.; and Woods, David C.: Preferential Concentration of Certain Elements in Smaller Aerosols Emitted From Aircraft Engines. J. Appl. Phys., vol. 46, no. 10, Oct. 1975, pp. 4590-4594.

2. Singh, Jag J.; Sentell, R. J.; and Khandelwal, G. S.: An Investigation of Size-Dependent Concentration of Trace Elements in Aerosols Emitted From the Oil-Fired Heating Plants. NASA TM X-3401, 1976.

3. Singh, Jag J.: Trace Elemental Characteristics of Aerosols Emitted From Municipal Incinerators. NASA TM-78630, 1978.

4. Keyser, T. R.; Natusch, D. F. S.; Evans, D. A., Jr.; and Linton, R. W.: Characterizing the Surfaces of Environmental Particles. Environ. Sci. & Technol., vol. 12, no. 7, July 1978, pp. 768-773.

5. Singh, Jag J.; and Khandelwal, G. S.: Elemental Characteristics of Aerosols Emitted From a Coal-Fired Heating Plant. NASA TM-78749, 1978.

6. Yue, Glenn K.; and Chan, L. Y.: The Formation of Ultrafine Aerosols Through Nucleation on Ions Process. Aerosole in Naturwissenschaft, Medizin und Technik - Dynamik und Nachweis ultrafeiner Aerosole, Gesellschaft für Aerosolforschung (GAF), [1979], pp. 9-14.

7. Yue, Glenn K.: A Quick Method for Estimating the Equilibrium Size and Composition of Aqueous Sulfuric Acid Droplets. J. Aerosol Sci., vol. 10, no. 1, Jan. 1979, pp. 75-86.

8. Yue, Glenn K.; and Chan, L. Y.: Theory of the Formation of Aerosols of Volatile Binary Solutions Through the Ion-Induced Nucleation Process. J. Colloid & Interface Sci., vol. 68, no. 3, Mar. 1979, pp. 501-507.

9. Yue, Glenn K.: On the Characteristics of Sulfate Aerosols Formed in the Presence of Ion Sources. J. Aerosol Sci., vol. 10, no. 4, July 1979, pp. 387-393.

10. Bricard, J; Cabane, M.; and Madelaine, G.: Formation of Atmospheric Ultrafine Particles and Ions From Trace Gases. J. Colloid & Interface Sci., vol. 58, no. 1, Jan. 1977, pp. 113-124.

11. Boulaud, D.; Madelaine, G.; Vigla, D.; and Bricard, J.: Experimental Study on the Nucleation of Water Vapor Sulfuric Acid Binary System. J. Chem. Phys., vol. 66, no. 11, June 1, 1977, pp. 4854-4860.

12. Mirabel, P.; and Clavelin, J. L.: Experimental Study of Nucleation in Binary Mixtures: The Nitric Acid-Water and Sulfuric Acid-Water Systems. J. Chem. Phys., vol. 68, no. 11, June 1, 1978, pp. 5020-5027.

13. Gmitro, John Irving; and Vermeulen, Theodore: Vapor-Liquid Equilibria for Aqueous Sulfuric Acid. A.I.Ch.E. J., vol. 10, no. 5, Sept. 1964, pp. 740-746.

14. Roedel, Walter: Measurement of Sulfuric Acid Saturation Vapor Pressure; Implications for Aerosol Formation by Heteromolecular Nucleation. J. Aerosol Sci., vol. 10, no. 4, July 1979, pp. 375-386.

15. Heist, R. H.; and Reiss, H.: Hydrates in Supersaturated Binary Sulfuric Acid-Water Vapor. J. Chem. Phys., vol. 61, no. 2, July 15, 1974, pp. 573-581.

16. Nair, P. V. N.; and Vohra, K. G.: Growth of Aqueous Sulphuric Acid Droplets as a Function of Relative Humidity. J. Aerosol Sci., vol. 6, nos. 3/4, June 1975, pp. 265-271.

17. Frazer, J. C. W.; Taylor, R. K.; and Grollman, A.: Two-Phase Liquid—Vapor Isothermal Systems, Vapor-Pressure Lowering. International Critical Tables of Numerical Data, Physics, Chemistry and Technology, Volume III, First ed., McGraw-Hill Book Co., Inc., 1928, pp. 292-300.

18. Weast, Robert C., ed.: Handbook of Chemistry and Physics. 56th ed. CRC Press, c.1975.

19. Searcy, J. Q.; and Fenn, J. B.: Clustering of Water on Hydrated Protons in a Supersonic Free Jet Expansion. J. Chem. Phys., vol. 61, no. 12, Dec. 15, 1974, pp. 5282-5288.

20. McKeown, Michael; and Siegel, Melvin W.: Atmospheric Pressure Ionization for Mass Spectrometry. American Lab., vol. 7, no. 11, 1975, pp. 89-92, 94, 96-99.

21. Kotake, S.; and Glass, I. I.: Survey of Flows With Nucleation and Condensation. AFOSR TR-79-0324, U.S. Air Force, Oct. 1978. (Available from DTIC as AD AO66 751.)

22. Peacock, G. R.: Methods of Measuring Sulfuric Acid Dewpoint. Analysis Instrumentation, Volume 15, J. F. Combs, F. D. Martin, and W. H. Wagner, eds., Instrum. Soc. America, 1977, pp. 9-16.

23. Tolman, Richard C.: Consideration of the Gibbs Theory of Surface Tension. J. Chem. Phys., vol. 16, no. 8, Aug. 1948, pp. 758-774.

24. Tolman, Richard C.: The Superficial Density of Matter at a Liquid-Vapor Boundary. J. Chem. Phys., vol. 17, no. 2, Feb. 1949, pp. 118-127.

25. Tolman, Richard C.: The Effect of Droplet Size on Surface Tension. J. Chem. Phys., vol. 17, no. 3, Mar. 1949, pp. 333-337.

TABLE I.- COMBINATIONS OF RELATIVE ACIDITY AND RELATIVE HUMIDITY UNDER WHICH CLUSTER SPECTRA WERE INVESTIGATED IN THE PRESENT STUDY

[Reaction chamber temperature ranged from 38.9 ± 0.1° C to 52.3 ± 0.1° C]

Number	Calculated R.A., percent	Measured R.H., percent (a)	Number	Calculated R.A., percent	Measured R.H., percent (a)
1	0.00047	7.5	17	0.00320	2.5
2	.00053	1.3	18	.00320	2.6
3	.00054	1.3	19	.00380	5.2
4	.00060	.7	20	.00440	1.4
5	.00060	1.4	21	.00442	1.4
6	.00060	1.8	22	.00450	1.5
7	.00100	1.6	23	.00460	1.5
8	.00105	.7	24	.00470	7.3
9	.00150	1.8	25	.00480	5.9
10	.00180	1.4	26	.00630	4.8
11	.00181	1.4	27	.00632	4.8
12	.00182	1.4	28	.00634	4.8
13	.00182	1.5	29	.01840	1.3
14	.00182	1.6	30	.03630	1.4
15	.00290	5.6	31	.04760	7.4
16	.00300	5.0	32	.06333	5.0

[a]The accuracy of the measured values of R.H. is determined almost entirely by the accuracy of the condensation mirror temperature sensor, which in the present instance was ±0.2° C.

TABLE II.- SUMMARY OF NUCLEATION CLUSTERS IN AN H_2SO_4 AND H_2O GAS MIXTURE

[R.A. = 0.0018 percent; R.H. = 1.6 percent]

(a) Experimental

Number	Cluster composition, $(H_2SO_4)_{N_A} \cdot (H_2O)_{N_B} \cdot H^+$	Relative intensity, percent
1	(5,x,1) x = 3,4,10,11,12,13	23.92
2	(1,x,1) x = 11,12,13	23.76
3	(2,x,1) x = 10,11,13	22.53
4	(4,x,1) x = 3,4,5,6,12,14	18.33
5	(3,x,1) x = 6,7,11	7.26
6	(6,x,1) x = 9,10	4.10

TABLE II.- Concluded

(b) Calculated[a]

Number	Cluster composition, $(H_2SO_4)_{N_A} \cdot (H_2O)_{N_B} \cdot H^+$	Probability, percent
1	1,2,1	39.61
2	1,3,1	28.07
3	1,1,1	8.76
4	2,2,1	7.21
5	2,3,1	5.69
6	1,4,1	4.91
7	2,1,1	3.43
8	2,4,1	1.62

[a]The calculated values are based on the following assumptions:

Effective cluster charge $Q = 1e$.

Effective cluster surface tension $\sigma = \sigma_{mac}$.

TABLE III.- SUMMARY OF CALCULATED CLUSTER CHARACTERISTICS AS A FUNCTION OF EFFECTIVE CLUSTER CHARGE

[R.A. = 0.0018 percent; R.H. = 1.6 percent; $\sigma = \sigma_{mac}$]

Number	Q = 1e		Q = 2e †	
	Cluster composition, $(H_2SO_4)_{N_A} \cdot (H_2O)_{N_B} \cdot H^+$	Probability, percent	Cluster composition, $(H_2SO_4)_{N_A} \cdot (H_2O)_{N_B} \cdot H^+$	Probability, percent
1	1,2,1	39.61	4,9,1	13.88
2	1,3,1	28.07	4,8,1	13.03
3	1,1,1	8.76	4,10,1	10.40
4	2,2,1	7.21	5,9,1	9.50
5	2,3,1	5.69	4,7,1	8.46
6	1,4,1	4.91	5,8,1	8.43
7	2,1,1	3.43	4,11,1	4.42
8	2,4,1	1.62	5,7,1	4.40
9			5,11,1	3.82
10			4,6,1	3.03
11			5,12,1	1.63

†The electrostatic term has been computed assuming a doubly charged spherical cluster.

TABLE IV.- SUMMARY OF CALCULATED[a] CLUSTER CHARACTERISTICS AS A FUNCTION OF EFFECTIVE SURFACE TENSION IN THE CLUSTER

[R.A. = 0.0018 percent; R.H. = 1.6 percent; Q = 1e]

Number	$\sigma = 1/2\ \sigma_{mac}$		$\sigma = 2\sigma_{mac}$	
	Cluster composition, $(H_2SO_4)_{N_A} \cdot (H_2O)_{N_B} \cdot H^+$	Probability, percent	Cluster composition, $(H_2SO_4)_{N_A} \cdot (H_2O)_{N_B} \cdot H^+$	Probability, percent
1	2,4,1	30.98	1,1,1	93.29
2	2,3,1	23.04	1,2,1	6.31
3	2,5,1	18.43	1,3,1	.15
4	1,3,1	5.42	2,1,1	.14
5	2,2,1	4.93		
6	2,6,1	4.61		
7	1,4,1	4.38		
8	1,2,1	1.41		
9	3,5,1	1.39		
10	1,5,1	1.37		
11	3,4,1	1.15		

[a]The clusters have been assumed to be singly charged spherical droplets.

TABLE V.- SUMMARY OF CALCULATED[a] CLUSTER CHARACTERISTICS

[R.A. = 0.0018 percent; R.H. = 1.6 percent; Q = 2e; $\sigma = 1/2\ \sigma_{mac}$]

Number	Cluster composition, $(H_2SO_4)_{N_A} \cdot H_2O)_{N_B} \cdot H^+$	Probability, percent
1	6,13,1	9.10
2	6,12,1	8.97
3	5,12,1	8.49
4	5,13,1	7.57
5	5,11,1	7.23
6	6,14,1	6.82
7	6,11,1	6.74
8	6,15,1	5.05
9	5,10,1	4.53
10	5,14,1	3.93
11	6,10,1	3.48
12	7,13,1	2.65
13	7,14,1	2.53
14	6,16,1	2.36
15	5,9,1	2.04
16	7,12,1	1.97
17	7,15,1	1.88
18	5,15,1	1.58
19	7,16,1	1.18
20	7,11,1	1.14
21	8,14,1	.25
22	8,15,1	.25

[a] The clusters have been assumed to be doubly charged spherical droplets.

TABLE VI.- SUMMARY OF CALCULATED CLUSTER GROUPS[a]

[R.A. = 0.0018 percent; R.H. = 1.6 percent; Q = 2e; $\sigma = 1/2\ \sigma_{mac}$]

Cluster group	Cluster composition, $(H_2SO_4)_{n_A} \cdot (H_2O)_{n_B} \cdot H^+$	Probability, percent
1	(5,x,1) x = 9,10,11,12,13,14,15	35.37
2	(6,x,1) x = 10,11,12,13,14,15,16	42.52
3	(7,x,1) x = 11,12,13,14,15,16	11.35
4	(8,x,1) x = 14,15	.50

[a]Most of the clusters predicted are outside the mass range of the detection system used. Only a few members of (5,x,1) and (6,x,1) cluster groups would be detected. However, secondaries produced by the fractionation of all the cluster groups predicted will be detected if their mass falls in the detectable range of the present system, 50 to 780 amu.

TABLE VII.- SUMMARY OF CALCULATED CLUSTER SPECTRA

DETECTABLE IN THE PRESENT STUDY

[R.A. = 0.0018 percent; R.H. = 1.6 percent;
Q = 2e; $\sigma = 1/2\ \sigma_{mac}$]

Cluster group	Cluster composition, $(H_2SO_4)_{N_A} \cdot (H_2O)_{N_B} \cdot H^+$	Relative intensity, percent
1	(5,x,1) x = 9,10,11,12,13,14,15	35.37
2	(6,x,1) x = 10,11	10.22

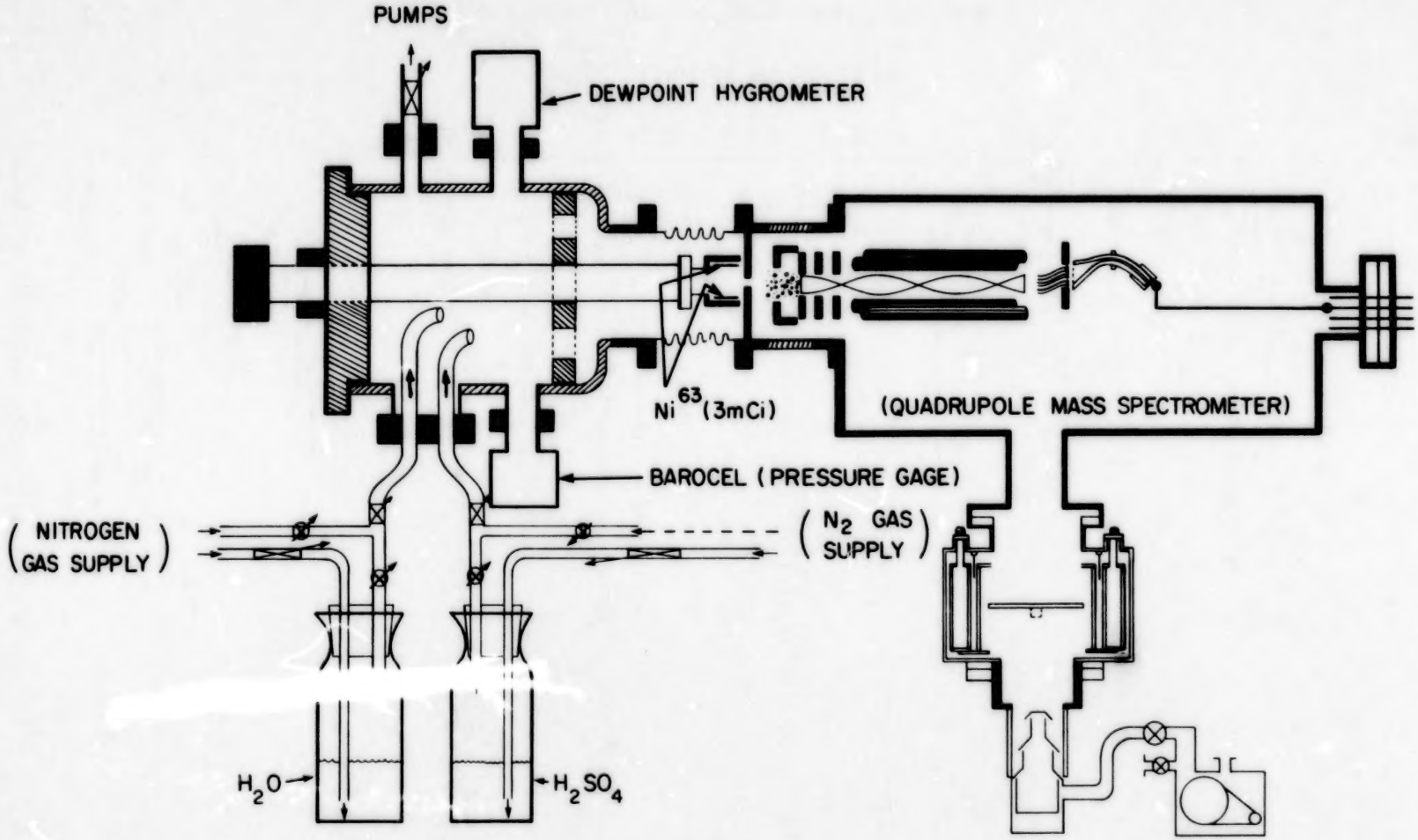

Figure 1.- Schematic diagram of experimental system used in study of ion-induced nucleation in (H_2O + H_2SO_4) gas mixture.

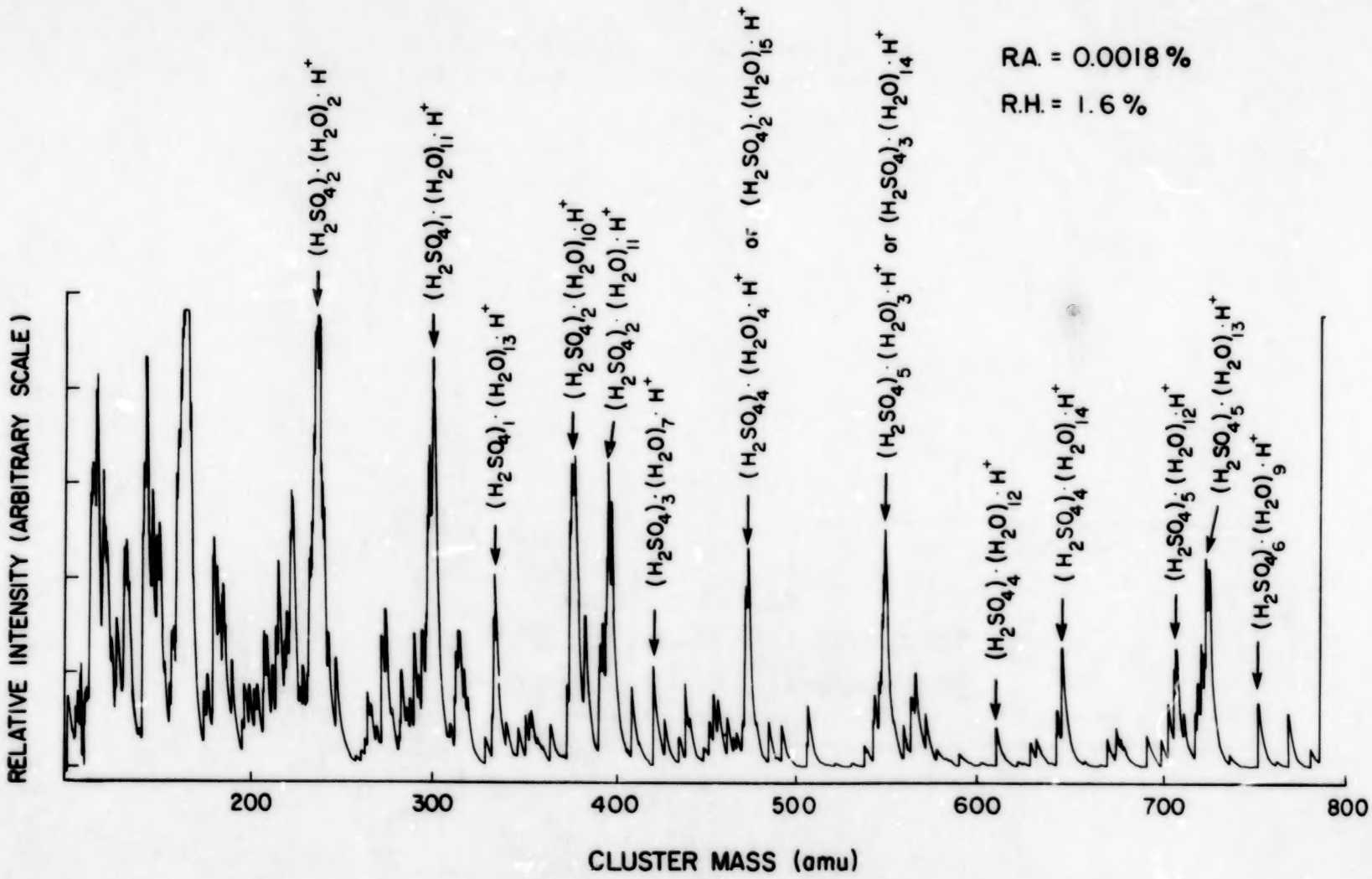

Figure 2.- Typical cluster mass spectrum.

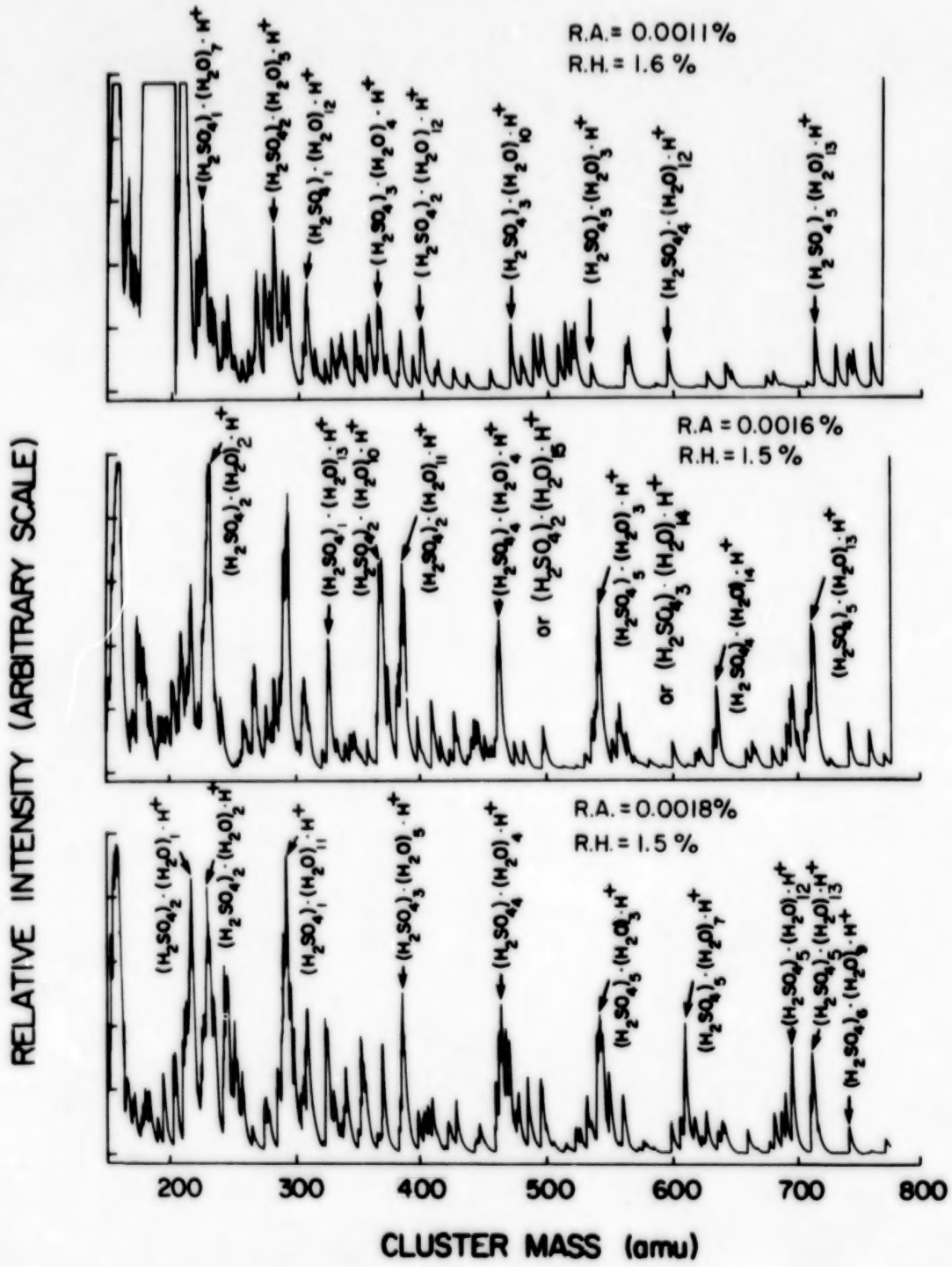

Figure 3.- Typical cluster spectra showing effect of decreasing R.A. on cluster spectrum.

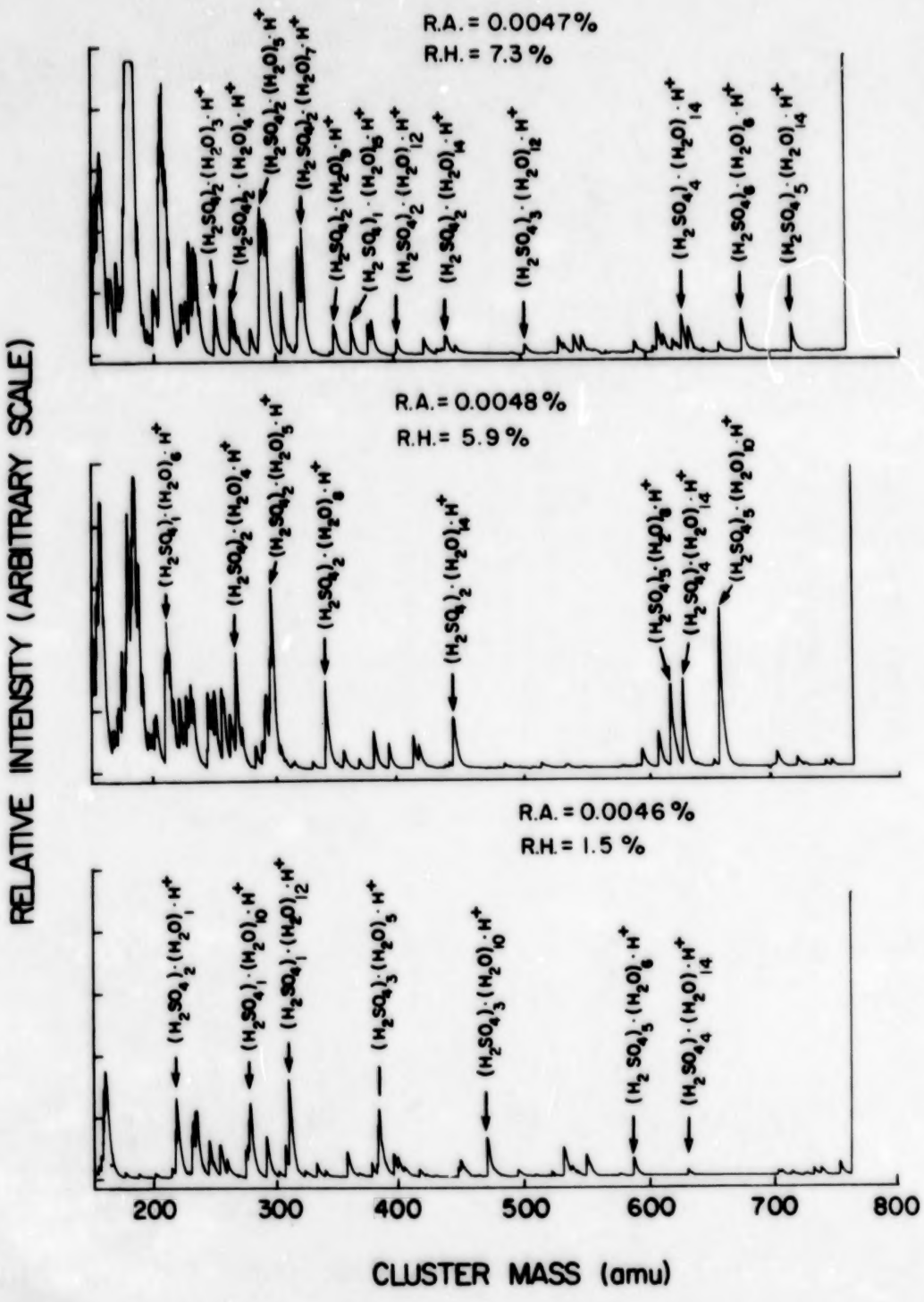

Figure 4.- Typical cluster spectra showing effect of increasing R.H. on cluster composition.

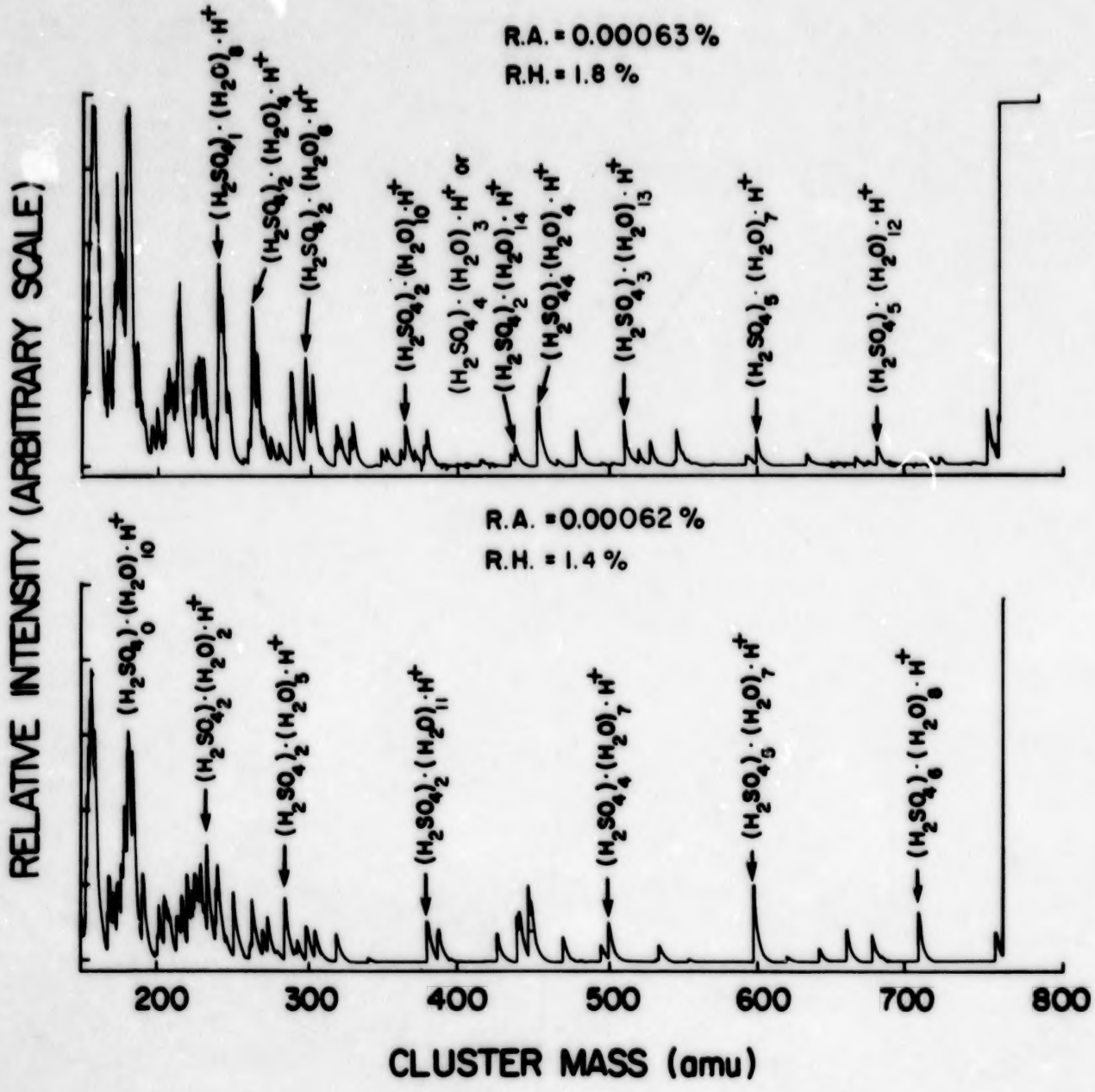

Figure 5.- Typical cluster spectra showing effect of a small increase in R.H. on cluster composition.

1. Report No. NASA TP-1735	2. Government Accession No.	3. Recipient's Catalog No.

4. Title and Subtitle	5. Report Date
EXPERIMENTAL STUDY OF CLUSTER FORMATION IN BINARY MIXTURE OF H_2O AND H_2SO_4 VAPORS IN THE PRESENCE OF AN IONIZING RADIATION SOURCE	November 1980
	6. Performing Organization Code

7. Author(s)	8. Performing Organization Report No.
Jag J. Singh, Alphonso C. Smith, and Glenn K. Yue	L-13878
	10. Work Unit No. 307-91-00-01
9. Performing Organization Name and Address NASA Langley Research Center Hampton, VA 23665	11. Contract or Grant No.
	13. Type of Report and Period Covered Technical Paper
12. Sponsoring Agency Name and Address National Aeronautics and Space Administration Washington, DC 20546	14. Sponsoring Agency Code

15. Supplementary Notes

Jag J. Singh and Alphonso C. Smith: Langley Research Center.
Glenn K. Yue: Institute for Atmospheric Optics and Remote Sensing, Hampton, Virginia.

16. Abstract

Molecular clusters formed in pure nitrogen containing H_2O and H_2SO_4 vapors and exposed to a 3-mCi Ni^{63} beta source have been studied in the mass range 50 to 780 amu using a quadrupole mass spectrometer. Measurements were made under several combinations of relative humidity and relative acidity ranging from 0.7 to 7.5 percent and 0.00047 to 0.06333 percent, respectively. The number of H_2SO_4 molecules in the clusters observed ranged from 1 to 7 whereas the number of H_2O molecules ranged from 1 to 16. The experimental cluster spectra differ considerably from those calculated using the classical nucleation theory. First-order calculations using modified surface tension values and including the effects of multipole moments of the nucleating molecules indicate that these effects may be enough to explain the difference between the measured and the calculated spectra.

17. Key Words (Suggested by Author(s))	18. Distribution Statement
Heteromolecular nucleation Molecular clusters H_2O and H_2SO_4 mixtures Ionizing radiation Microscopic surface tension Distributed charges Quadrupole mass spectrometer	Unclassified - Unlimited Subject Category 45

19. Security Classif. (of this report)	20. Security Classif. (of this page)	21. No. of Pages	22. Price
Unclassified	Unclassified	27	A03

For sale by the National Technical Information Service, Springfield, Virginia 22161

NASA-Langley, 1980

END

12/15/80